Chiral Ordering in Supercooled Liquid Water and Amorphous Ice

Masakazu Matsumoto, Takuma Yagasaki, and Hideki Tanaka
Graduate School of Natural Science and Technology, Okayama University, 3-1-1 Tsushima, Okayama 700-8530, Japan
(Received 26 May 2015; published 5 November 2015)

The emergence of homochiral domains in supercooled liquid water is presented using molecular dynamics simulations. An individual water molecule possesses neither a chiral center nor a twisted conformation that can cause spontaneous chiral resolution. However, an aggregation of water molecules will naturally give rise to a collective chirality. Such homochiral domains possess obvious topological and geometrical orders and are energetically more stable than the average. However, homochiral domains cannot grow into macroscopic homogeneous structures due to geometrical frustrations arising from their icosahedral local order. Homochiral domains are the major constituent of supercooled liquid water and the origin of heterogeneity in that substance, and are expected to be enhanced in low-density amorphous ice at lower temperatures.

DOI: 10.1103/PhysRevLett.115.197801 PACS numbers: 61.20.Ja, 64.60.My, 64.70.pm, 81.07.Nb

When liquid water is supercooled at ambient pressure, its properties are expected to approach those of low-density amorphous ice (LDA), which is characterized by low enthalpy, low entropy [1], low mobility, and a locally tetrahedral configuration of the molecules. These characteristics are often referred to as being "icelike." Many microscopic indices such as the coordination number [2], the bond orientational order [3], and the local structure index [4], etc., also become "icelike." Most anomalies in water emerge at this temperature range. Much effort has therefore been devoted to elucidating the properties of the supercooled liquid water. However, our knowledge of the structure and properties of this substance is still limited.

Dynamical and structural heterogeneities emerge when liquid water is supercooled deeply [4–6]. This phenomenon is often discussed in relation to the hypothetical liquid–liquid critical point of water [7,8]. In the context of glass transition phenomena, these heterogeneities are characteristic to supercooled liquids, in general [9], attributed to the locally stable structures [10], and probably, related to the crystallization [11,12], but not necessarily to liquid–liquid coexistence. Moreover, in the case of liquid water, it has been argued that the liquid–liquid separation is just a transient, coarsening process toward crystal ice [13]. Other researchers have argued that a heterogeneous structure of hypothetical metastable ice prevails in the deeply supercooled liquid water, and it assists ice nucleations [14]. These inconsistent viewpoints come from the fact that the structure of LDA has not been well characterized. All ice crystals as well as relaxed LDA are locally tetrahedrally coordinated. Indices including the coordination number and the local structure index cannot distinguish topological differences in the hydrogen bond network of ice. The existence of intermediate-range order (IRO) in the supercooled liquid water has been suggested in much of the literature based on the orientational order [15,16], many-body correlation function [17], and spaciotemporal correlations [18], etc., but direct evidence is lacking.

In this Letter, we perform an exhaustive topological search of local structures to find the genuine origin of the "icelikeness." Our method can distinguish the structures of all stable and metastable ice phases at low pressure as well as even the locally stable structures of liquids. This method has previously been used to explain the structure change when liquid water is supercooled and expands [19]. In the present Letter, we utilize this method for a more comprehensive classification of the local structures in the supercooled liquid water.

Constant temperature and pressure molecular dynamics simulations are performed for 3 μs with 8,000 water molecules of the TIP4P/2005 model [20] using the GROMACS software [21]. A cubic cell is used. Pressure is maintained at 1 atm. Detailed analyses are made at intervals of 10 K between 200 and 240 K, which are about 50 and 10 K below the melting point of TIP4P/2005 water, respectively [22]. At these conditions, liquid water neither vitrifies nor crystallizes within 3 μs. Two water molecules are regarded as being hydrogen bonded when the intermolecular H-O distance is below 2.45 Å [23]. In the calculation of the chirality and searching vitrites, the direction of the hydrogen bond (HB) is ignored.

One simple measure of IRO for tetravalent network-forming materials is the torsional angle of a bond connecting two tetrahedral sites. Water molecules tend to have a locally tetrahedral configuration, which gives rise to a preference in the conformations of dihedral angles [24] similar to alkanes. We therefore define the "bond twist" for a given HB by the following formula:

$$\chi_b = \frac{1}{lm}\sum_{i=1}^{l}\sum_{j=1}^{m}\tau_{ij}, \tag{1}$$

where i and j specify the other HBs connected to the two ends of the given HB (three bonds for each in ices) and $\tau_{ij} = \sin 3\theta_{ij}$ is the twist at a dihedral angle θ_{ij} [25] (Inset of Fig. 1). Note that l and m are not always 3 in liquids. A dihedral angle is defined by centers of mass of four successive water molecules connected by HBs. The twist, τ, becomes its extremal values, ± 1, when the angles are $120n \pm 30°$, respectively, whereas it is 0 for all dihedral angles in six- and seven-membered rings in boat or chair conformations. Therefore, τ and χ_b are 0 for ideal cubic and hexagonal ices I (ices Ic and Ih) [26]. τ takes various values in liquid water reflecting its randomness. The distribution of χ_b is therefore broad near the melting point (Fig. 1). However, the distribution has a central peak because the distortion of the local configuration from a regular tetrahedron causes cancellation of the twists. Conversely, in deeply supercooled liquid water, almost-regular tetrahedral configuration prevents the cancellations of the twists, and the distribution of χ_b becomes much broader; i.e., the distribution does not approach that of ice unlike other popular structural indices (Fig. 1). This wide distribution of χ_b is a property specific to supercooled liquid water and LDA ice.

The topology of the HB network of water strongly affects the physical properties of liquid water and ice. Supercooled liquid water at ambient pressure exhibits a hierarchical IRO in its network starting from a locally tetrahedral configuration to four-site chains (dihedral angle), rings (mainly five to seven membered), polyhedral structures, and aggregations of polyhedral structures [27]. We shall therefore examine the twists in each class of IRO.

First of all, we define the ring twist as the averaged twist along the n-membered ring R,

$$\chi_r = \frac{1}{n}\sum_{i\in R}^{n} \sin 3\theta_i, \tag{2}$$

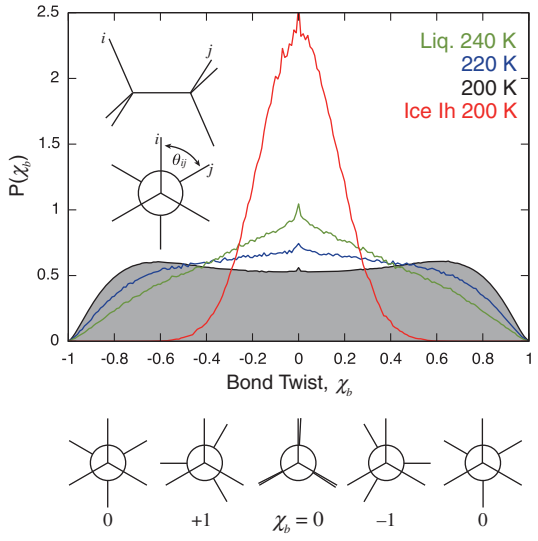

FIG. 1 (color). Distributions of bond twists, χ_b, for supercooled liquid water and ice. The melting temperature of the employed model is approximately 250 K.

where θ is the dihedral angle for a four-molecule chain along the ring. The distribution of χ_r is centered at $\chi_r = 0$ because twists in a ring cancel each other in most cases. It is, however, still broader at lower temperatures (Fig. 2). We find that the HB network of supercooled liquid water mostly comprises five- to seven-membered rings and that the six-membrered ring is responsible for the broadening [Fig. 2(b)]. All known stable and metastable ices at low pressures (Ih, Ic, and XVI [28]) as well as clathrate hydrates have rings of $\chi_r = 0$ only; these rings do not contribute to the broadening. (See Supplemental Material [29] for other hypothetical metastable ice polymorphs.)

As a larger-scale IRO than those that can be described by ring statistics, we introduce polyhedral unit structures comprising several rings in liquid water and ice. Ice and clathrate hydrate structures at low pressures can be visually recognized as a combination of one or two types of polyhedral building blocks, a.k.a. "crystallites" [Fig. 3(a)]. The building blocks all comprise five- or six-membered rings, and contain a void inside. It has been suggested that similar cagelike structures are also abundant in supercooled liquid water [2]. We therefore gave a general topological definition of such polyhedral building blocks comprising

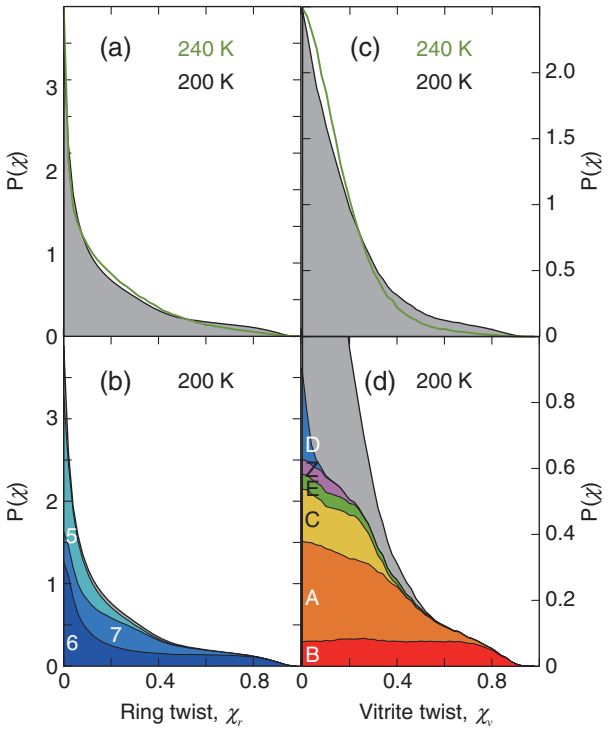

FIG. 2 (color). Distribution of ring twists. (a) Overall distribution of the ring twists, χ_r, at 200 K (black) and 240 K (green). (b) Contributions of five- to seven-membered rings to the distribution at 200 K are shown with a stacked chart. The probability is defined on a per-ring basis. See Supplemental Method [29] for detail. (c) Overall distribution of the vitrite twist at 200 K (black) and 240 K (green). (d) Lower part of panel (c) at 200 K is expanded and the contributions from major types of vitrites are shown.

rings in a previous work [27]. In fact, the HB network of deeply supercooled liquid water is full of five- to seven-membered rings, and we found that the network can be tessellated into cages of various types in a manner similar to ice and hydrates. We call these polyhedral building blocks "vitrite" because they constitute the greatest part of low-density amorphous ice [27]. (This is also illustrated in Fig. S1; definition of vitrites is also given in the Supplemental Method [29].) We also defined a "cluster" as a face-sharing aggregate of the vitrites. A dihedral angle is defined for a chain of four successive water molecules connected by three hydrogen bonds, and one can find many chains in a vitrite. We define the vitrite twist, χ_v, as the averaged twist for all dihedral angles in a vitrite V:

$$\chi_v = \frac{1}{n}\sum_{i\in V}^{n} \sin 3\theta_i, \tag{3}$$

where n is the total number of such chains in a vitrite. As shown in Fig. 2(c), χ_v also becomes broader at lower temperatures. We find that vitrites A and B are the most and second most abundant vitrites. Moreover, these vitrites are also responsible for the broadening of the vitrite twist distribution for $|\chi_v| > 0.5$ [Fig. 2(d)].

Vitrite B comprises three six-membered rings. An alternate arrangement of vitrites B and H that shares the six-membered rings of a boat conformation results in ice Ih structure [Fig. 3(a)]. Conversely, one can attach type B vitrites together by sharing the six-membered rings in a twisted-boat conformation to build a single-component cluster of vitrite B [Fig. 3(b); also illustrated in Fig. S2]. This structure, built of six-membered rings only, was first proposed as a model of tetravalent amorphous semiconductors and named "polytope '240'" [34], and was later suggested as a possible locally stable structure of water [2,35,36]. The structure can also be built by decorating (i.e., regularly inserting vertices to) an icosahedral close-packing cluster [Fig. 3(b)]. There are two symmetric ways to make the surface hexagonal rings of type B vitrite twisted-boat conformations without introducing large distortions [illustrated in Fig. 3(d)]; let us call them right and left twists. When a vitrite B is right twisted, the χ_r values of all three hexagonal rings as well as χ_v positively deviate from zero. A left twist results in negative deviations. Because a right-twisted hexagonal ring cannot overlap with a left-twisted one, only vitrites B of the same twist (right or left) can attach to one another by sharing their twisted surface rings. Thus, the aggregation of type B vitrites naturally gives rise to the homochiral domain. However, note that the geometrical frustration by icosahedral symmetry [34] prevents polytope '240' from growing into an infinitely large aggregate without defects (i.e., crystal).

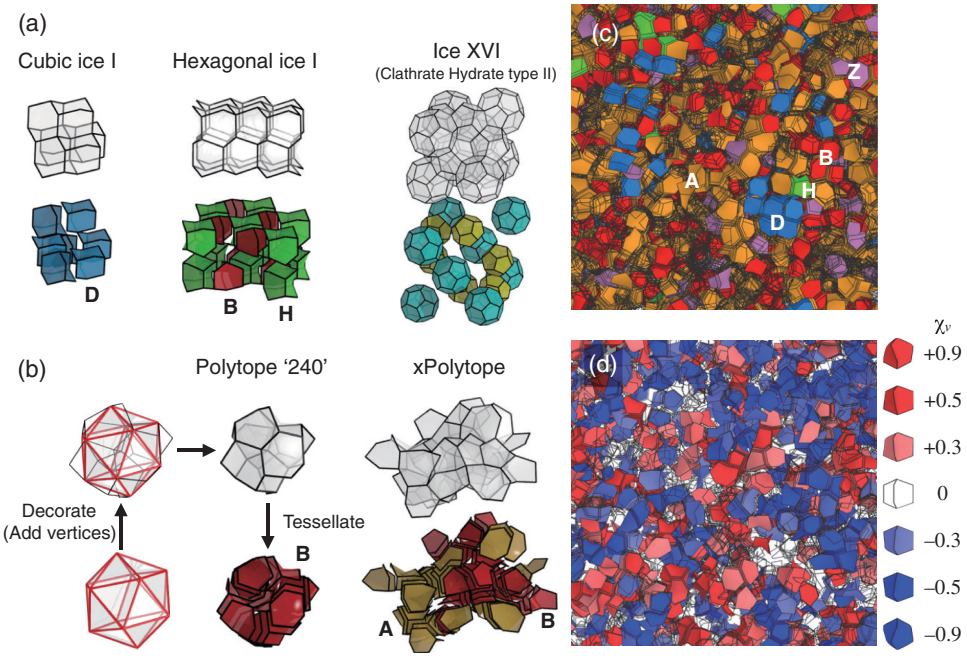

FIG. 3 (color). Vitrites in ice and in supercooled water. (a) Various stable and metastable ice structures can be decomposed into vitrites (crystallites). Major vitrite types B, D, and H are labeled. (b) An icosahedron comprises 20 almost-regular tetrahedra. Polytope '240' structure is made from an icosahdron by regularly inserting vertices at the centers of one fifth of the tetrahedra and can also be decomposed into several type B vitrites. XPolytope is an aggregate of vitrites A and B. (c) A snapshot of the entire system of the supercooled liquid water at 200 K is decomposed into vitrites. Vitrite types A, B, D, H, and Z are shown with filled polyhedra and other types are shown with outlines. Label D points the largest ice Ic nucleus that appears in the trajectory. Abundance of each vitrite type is listed in Table S1. (d) Vitrite types A and B (xPolytope) are gradated from blue to red according to their twists, χ_v, in the same snapshot used in panel c. Only the vitrites with $|\chi_v| > 0.25$ are shown with filled polyhedral and others are shown with outlines.

Another major vitrite, type A, is derived from B by adding a vertex. The vitrite comprises a six-membered ring and two seven-membered rings. Two type-A vitrites join each other by sharing their surface rings, and vitrite A also gets twisted when it shares the six-membered ring with the polytope '240'. The combination contributes to a relaxation of the frustration of the polytopic structure and an extension of the homochiral domain. We define an extended polytopic cluster, "xPolytope", as a cluster of two or more vitrites A and B having the same chirality with a threshold of $|\chi_v| > 0.25$. The mole fractions of water molecules belonging to any xPolytope are 3% at 240 K and 14% at 200 K (Fig. 4.).

XPolytope stabilizes the local structure of supercooled water. To clarify this point, we count the number of vitrites sharing a given HB. For example, each HB in the bulk ice Ic structure belongs to six type-D vitrites. We express this "multiplicity" as $M(\mathrm{D}) = 6$. Similarly, $M(\mathrm{B}) = 9$ for each HB in an ideal polytope '240' (See Fig. S3). In liquid water, M varies for each HB and for different vitrite types. At 200 K, a HB belongs to 1.5 vitrites A or B on average, i.e., $\bar{M}(A \text{ or } B) = 1.5$. Figure 5(a) shows the relationship between M and the stability of the local structure. With increasing $M(\mathrm{D})$, i.e., as the environment of the HB becomes more icelike, molecular motions are suppressed and the potential energy decreases. The suppression of molecular motions and the decrease in potential energy with increasing multiplicity are also observed for vitrites A and B. This indicates that the clustering of vitrites A and B is energetically and dynamically similar to that of the fragment of ice Ic, vitrite D. Note that the aggregation of A and B is quite different from that of D in terms of chirality. The distribution of bond twists becomes narrower with increasing $M(D)$, whereas it becomes distinctly bimodal at high $M(A \text{ or } B)$ (Fig. S4).

The XPolytope is stable and comprises a few types of vitrites like a crystal does. In fact, it even nucleates in supercooled liquid water. At 200 K, a ice Ic nucleus, identified as an aggregate of vitrite D, rarely appears [Figs. 3(c) and 5(b)]. It occasionally grows up to a few nanometers in diameter, persists for tens of nanoseconds, and then disappears. Similar intermittent growth and annihilation also occur for xPolytope. Figure 5(b) shows that the sizes of the left- and right-twisted clusters change independently. The cluster size distributions of ice Ic and xPolytope are shown in Fig. 5(c). The latter is larger than the former at all temperatures, and their temperature dependence suggests that the ratio of the volume occupied by xPolytope to that by ice Ic would be larger in LDA at lower temperatures than in

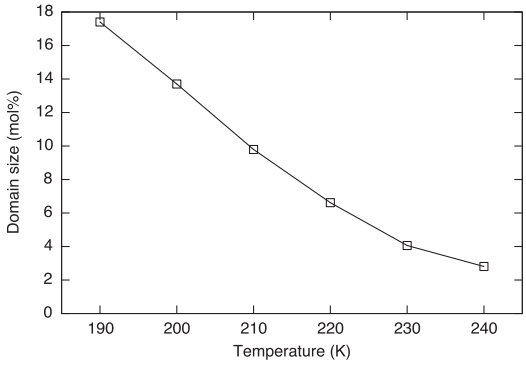

FIG. 4. The mole fraction of water molecules belonging to any xPolytope is plotted against temperature.

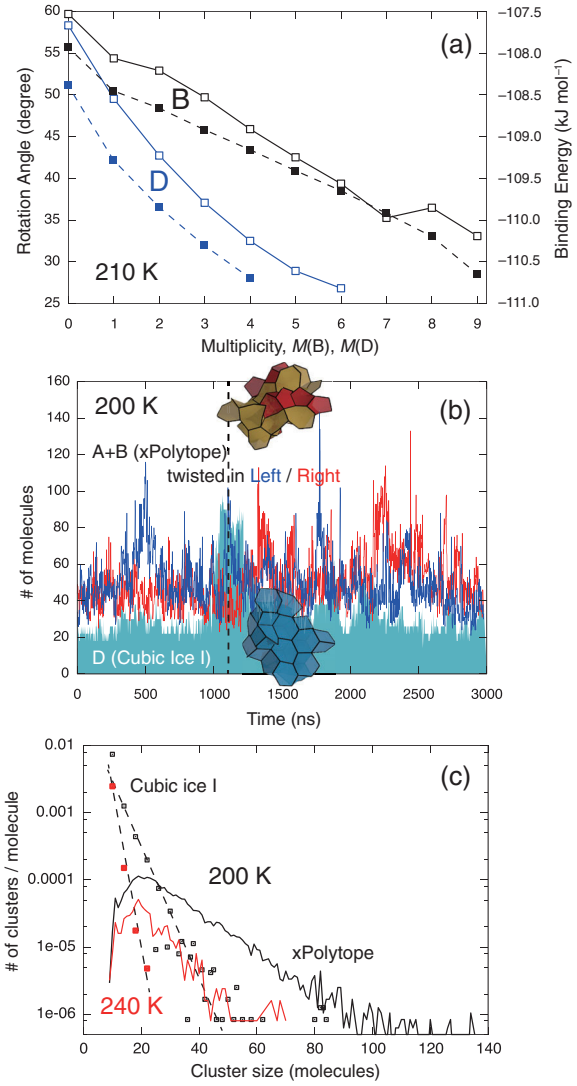

FIG. 5 (color). Correlation between structure, dynamics, and chirality. (a) Solid and dashed lines show the averaged rotation angles in 2 ns and the averaged binding energies of two water molecules constituting a hydrogen bond, respectively, as functions of multiplicities $M(D)$ (blue lines, ice Ic) and $M(B)$ (black lines, polytope '240'). (b) Size of the largest cluster at 200 K plotted against time. Red and blue lines are for xPolytopes with $\chi_v > 0.25$ and $\chi_v < -0.25$, respectively. Light blue is for the nucleus of ice Ic (vitrite D). Inserted are the shapes of the largest clusters at 1,114 ns (indicated by a dashed line), which is the same instant shown in Figs. 3(c) and 3(d). A large ice nucleus appears at 1 μs and persists for 300 ns. (c) Cluster size distributions at 240 K (red) and 200 K (black). Dots and solid lines indicate ice Ic and xPolytope, respectively.

supercooled water at 200 K. Thus, the homochiral domain found in this study is not just a random percolation cluster of major vitrite types, but a stable self-organizing structure comprising structural, dynamic, and chiral heterogeneity.

Polytope '240' structure was considered as a model for tetravalent amorphous semiconductors; however, no surveys have been made for amorphous ice and supercooled liquid water. As shown in this Letter, xPolytopes grow up to much larger nuclei than the original polytopes '240' do due to a heterogeneous element, vitrite *A*. Moreover, xPolytopes are the origin of collective chirality in supercooled water. Molecular arrangements of xPolytope are twisted; therefore, they do not seem to have affinity to crystal ice structures with untwisted molecular arrangements. The growth of polytopic domain may disturb crystallization by reducing the space for ice nucleation.

Unlike ice nuclei, xPolytope is abundant in liquid water at temperatures close to the melting point [Fig. 5(c)]. Its appearance may be controlled by external fields such as impurity, surfaces, etc. Interestingly, polytopic aggregate has also been observed in the vicinity of collagen molecules at room temperature [37]. This coincidence suggests that the vicinal water is not icelike but LDA-like and that chirality will be helpful for detecting structured water [38,39]. Their domain size may be enhanced by low temperatures, surfaces, impurities, and long relaxation times, etc., and the amorphous ice in comets satisfies all these conditions. Experiments assuming the cometary circumstances and fine observation of nanoscale chirality in amorphous ice are, therefore, awaited. The present research redefines the icelikeness of supercooled liquid water, elucidates the intermediate-range order in liquid water, provides a new way of analyzing the liquid and crystal structures, and suggests a novel interaction between water structure and biomolecules through the chirality.

Professor Kenji Mochizuki and Mr. Tatsuya Nakamura are acknowledged for discussions and proof reading. The present work was supported by a Grant-in-Aid by JSPS (Grant No. 25288008) and by HPCI Strategic Programs for Innovative Research (SPIRE) and Computational Materials Science Initiative (CMSI), MEXT, Japan. Calculations were performed at Research Center for Computational Science (RCCS), Okazaki, Japan.

[1] M. A. Floriano, Y. P. Handa, D. D. Klug, and E. Whalley, J. Chem. Phys. **91**, 7187 (1989).
[2] F. H. Stillinger, Science **209**, 451 (1980).
[3] H. Tanaka, Phys. Rev. E **62**, 6968 (2000).
[4] E. Shiratani and M. Sasai, J. Chem. Phys. **108**, 3264 (1998).
[5] E. La Nave and F. Sciortino, J. Phys. Chem. B **108**, 19663 (2004).
[6] J. R. Errington, P. G. Debenedetti, and S. Torquato, Phys. Rev. Lett. **89**, 215503 (2002).
[7] P. H. Poole, F. Sciortino, U. Essmann, and H. E. Stanley, Nature (London) **360**, 324 (1992).
[8] J. C. Palmer, F. Martelli, Y. Liu, R. Car, A. Z. Panagiotopoulos, and P. G. Debenedetti, Nature (London) **510**, 385 (2014).
[9] P. G. Debenedetti and F. H. Stillinger, Nature (London) **410**, 259 (2001).
[10] A. Ha, I. Cohen, X. Zhao, M. Lee, and D. Kivelson, J. Phys. Chem. **100**, 1 (1996).
[11] R. S. Singh and B. Bagchi, J. Chem. Phys. **140**, 164503 (2014).
[12] T. Kawasaki and H. Tanaka, J. Phys. Condens. Matter **22**, 232102 (2010).
[13] D. T. Limmer and D. Chandler, J. Chem. Phys. **138**, 214504 (2013).
[14] J. Russo, F. Romano, and H. Tanaka, Nat. Mater. **13**, 733 (2014).
[15] P. Kumar, G. Franzese, S. V. Buldyrev, and H. E. Stanley, Phys. Rev. E **73**, 041505 (2006).
[16] D. P. Shelton, J. Chem. Phys. **141**, 224506 (2014).
[17] D. Dhabal, M. Singh, K. T. Wikfeldt, and C. Chakravarty, J. Chem. Phys. **141**, 174504 (2014).
[18] B. Jana and B. Bagchi, J. Phys. Chem. B **113**, 2221 (2009).
[19] M. Matsumoto, Phys. Rev. Lett. **103**, 017801 (2009).
[20] J. L. F. Abascal and C. Vega, J. Chem. Phys. **123**, 234505 (2005).
[21] B. Hess, C. Kutzner, D. van der Spoel, and E. Lindahl, J. Chem. Theory Comput. **4**, 435 (2008).
[22] R. G. Fernández, J. L. F. Abascal, and C. Vega, J. Chem. Phys. **124**, 144506 (2006).
[23] M. Matsumoto, J. Chem. Phys. **126**, 054503 (2007).
[24] M. Mezei and R. J. Speedy, J. Phys. Chem. **88**, 3180 (1984).
[25] D. P. DiVincenzo and M. H. Brodsky, J. Non-Cryst. Solids **77–78**, 241 (1985).
[26] H. Tanaka and I. Okabe, Chem. Phys. Lett. **259**, 593 (1996).
[27] M. Matsumoto, A. Baba, and I. Ohmine, J. Chem. Phys. **127**, 134504 (2007).
[28] A. Falenty, T. C. Hansen, and W. F. Kuhs, Nature (London) **516**, 231 (2014).
[29] See Supplemental Material at http://link.aps.org/supplemental/10.1103/PhysRevLett.115.197801, which includes Refs. [30–33], for definitions of hydrogen bond and vitrite, discussion on the appearance frequencies of various vitrites, the model independency, the structure of polytope '240', etc.
[30] M. Matsumoto, A. Baba, and I. Ohmine, AIP Conf. Proc. **982**, 219 (2008).
[31] T. Yagasaki, M. Matsumoto, and H. Tanaka, Phys. Rev. E **89**, 020301 (2014).
[32] C. J. Fennell and J. D. Gezelter, J. Chem. Theory Comput. **1**, 662 (2005).
[33] F. W. Starr, J. K. Nielsen, and H. E. Stanley, Phys. Rev. E **62**, 579 (2000).
[34] R. Mosseri, D. P. DiVincenzo, J. F. Sadoc, and M. H. Brodsky, Phys. Rev. B **32**, 3974 (1985).
[35] J. Kolafa and I. Nezbeda, Mol. Phys. **84**, 421 (1995).
[36] N. A. Bulienkov, J. Mol. Liq. **106**, 257 (2003).
[37] E. Rubtcova, A. Solovey, and V. Lobyshev, in *Chemical and Biochemical Technology* (Apple Academic Press, New Jersey, 2014), p. 13.
[38] P. Kumar, Z. Yan, L. Xu, M. G. Mazza, S. V. Buldyrev, S. H. Chen, S. Sastry, and H. E. Stanley, Phys. Rev. Lett. **97**, 177802 (2006).
[39] M. G. Mazza, K. Stokely, S. E. Pagnotta, F. Bruni, H. E. Stanley, and G. Franzese, Proc. Natl. Acad. Sci. U.S.A. **108**, 19873 (2011).